Theoretical Modelling and Experimental Verification of the Heat Transfer Behaviour of a Water-charged Closed-end Loop Pulsating Heat Pipe

G. Swanepoel, R.T. Dobson[*] & A.B. Taylor

Department of Mechanical Engineering, University of Stellenbosch, Private Bag X 1, Matieland, 7602, South Africa

Abstract

In this paper the theoretical modelling of a Pulsating Heat Pipe (PHP) is presented. In this particular model the flow of the working fluid is modelled as discrete liquid plugs moving back and forth because of the evaporation and condensation processes taking place inside of the PHP. A PHP was manufactured to determine the heat transfer rate of the PHP experimentally and to compare the experimental results with the theoretical results. The average heat transfer rate predicted by the theoretical model in the top heat mode was 62 W compared to the experimental value of 60 W. In the bottom heat mode the average theoretical predicted heat transfer rate was 86 W compared to the experimental determined value of 65W.

Keywords: pulsating heat pipes, evaporation of liquid film, accommodation coefficient, capillary force, contact angle

Nomenclature

A Area [m^2]

d diameter [m]

C_f friction factor (Fanning)

c_v specific heat at constant volume [J/kgK]

c_p specific heat at constant pressure [J/kgK]

F force [N]

g gravitational constant [m/s^2]

h heat transfer coefficient [W/m^{2}K]

i enthalpy, [J/kgK]

i_{fg} latent heat of vaporization, [J/kg]

L length [m]

m mass [kg]

$\dot{m}''$ mass flux [kg/m^{2}s]

n number

p pressure [N/m^2]

$\dot{Q}$ heat transfer rate, power [W]

R specific gas constant [J/kgK], filling ratio

Re Reynolds number

T temperature [°C]

t time [s]

U internal energy [J], overall heat transfer coefficient [W/m^{2}K]

V volume [m^3]

v velocity [m/s]

W width [m]

x   distance [m]

$\dot{x}$ velocity [m/s]

Greek letters

δ thickness [m]

ϕ inclination angle [°]

* Corresponding Author. Tel.: +27 (0)21 808 4268, Fax.: +27 (0)21 808 4958, email.: rtd@maties.sun.ac.za

μ viscosity [Pas]

θ contact angle [°]

ρ density [kg/m^3]

σ surface tension [N/m]

τ shear stress [N/m^2]

Subscripts

a   advancing

c   cross section, condensation, capillary

chan   channels

elec   electrical

f   friction

i   inner

ℓ liquid

ℓf liquid film

max   maximum

mod   modified

o   outer

p   plug

r   receding

sat   saturated

v   vapour

w   wall

1. Introduction

A Pulsating Heat Pipe (PHP) consists of a long meandering tube filled with a working fluid

as shown in Fig. 1. The internal diameter of the tube is in the region of the capillary length,

3

given by $L = \left(\sigma / (\rho_\ell - \rho_v) g \right)^{0.5}$. The small inside diameter and surface tension discrete cause liquid plugs and vapour bubbles to co-exist. In the heated section evaporation takes place causing the pressure in the vapour bubbles to increase. This increase in pressure in the vapour bubbles causes pressure differentials across some of the liquid plugs, causing some of the liquid plugs to move. In the cooled section condensation takes place causing the pressure to decrease in the vapour bubbles. These decreases in pressure also causes pressure differentials across some of the liquid plugs causing those plugs to move as well. Due to the fact that all the liquid plugs and vapour bubbles are interconnected by a single tube the movement of any plug will cause neighbouring liquid plugs to move as well, causing all the liquid plugs to oscillate in an apparently irregular aperiodic manner. The liquid plugs do not move as discrete entities all the time and some of the liquid plugs can coalesce to create a single plug or some split up to form two separate liquid plugs.

For the theoretical model the PHP is modelled as a straight tube of a length L_{tube}, inside diameter d_i and outside diameter d_o, containing several liquid plugs with a vapour bubble at each end of a liquid plug, as shown in Fig. 2. This is similar to previous models by Dobson and Harms [1] and Swanepoel et al. [2], which is in contrast to other approaches, such as that by Maezawa et al. [3], where the fluid flow is considered as a homogenous mixture of vapour and liquid with the quality varying depending on the heat transfer. Portions of the tube may be heated, cooled or insulated and a liquid film of varying thickness $\delta_{\ell f}$ may be present on the inner wall of the tube. For a portion of the wall covered with a liquid film, heat may be transferred from the tube wall to the liquid film. The temperature of the liquid film then increases causing evaporation to take place. The portion of the liquid film that evaporates enters the adjacent vapour bubble causing the mass and the internal energy of that vapour bubble to increase. For portions of the wall not covered with a liquid film, heat is directly

4

transferred from the wall to the vapour bubble for the case where the wall is hotter than the vapour bubble and vice versa. If the wall is cooler than the vapour bubble, condensation can take place causing a liquid film to form on the tube wall. The increase in the mass and internal energy of the vapour bubble causes the pressure in the vapour bubble to increase. The change in pressure is not the same for all the vapour bubbles so that a situation arises where the vapour pressure difference across a liquid plug causes the plug to move. As the liquid plug moves it experiences a frictional shear stress exerted by the tube wall, a force caused by the capillary pressure that exists across the liquid plug due to surface tension and a gravitational force.

2. Derivation of Governing Equations of Change

Consider the vapour bubble between the two liquid plugs as shown in the squared area of the tube in Fig. 2, shown enlarged in Fig. 3. Fig. 4 shows the heat transfer between the wall and the vapour bubble, the liquid film and the vapour bubble and the energy transfer due to mass transfer. Also shown is the work done by the vapour bubble as it expands. An energy balance on the vapour bubble gives

$$\frac{dU_v}{dt} = h_{wv} A_v (T_w - T_v) + h_{\ell fv} A_{\ell f} (T_{\ell f} - T_v) + \dot{m}''_{\ell f} A_{\ell f} i_v - \dot{m}''_{wv} A_v i_v - p_v \frac{dV_v}{dt}$$

(1)

where

$$\frac{dU_v}{dt} = m_v c_{vv} \frac{dT_v}{dt}, \ A_v = \pi d_i L_v, \ A_{\ell f} = \pi d_i L_{\ell f}, \ m_v = \rho V_v \text{ and } V_v = \tfrac{1}{4} \pi d_i^2 (L_{\ell f} + L_v)$$

(Note that the effect of the thickness of the liquid film is ignored in determining the contact area between the vapour bubble and the liquid film as well as the vapour bubble volume)

A mass balance on the liquid film shown in Fig. 5(a) gives

$$\frac{dm_{\ell f}}{dt} = -\dot{m}''_{\ell f} A_{\ell f}$$

(2)

where $m_{\ell f} = \rho_{\ell f} L_{\ell f} \frac{1}{4}\pi\left(d_i^2 - (d_i - 2\delta_{\ell f})^2\right)$

A mass balance on the vapour bubble shown in Fig. 5(b) gives

$$\frac{dm_v}{dt} = \dot{m}''_{\ell f} A_{\ell f} - \dot{m}''_{wv} A_v$$

(3)

where $m_v = \rho V_v$, $V_v = \frac{1}{4}\pi d_i^2\left(L_{\ell f} + L_v\right)$, $A_{\ell f} = \pi d_i L_{\ell f}$ and $A_v = \pi d_i L_v$

Consider a liquid plug of mass m_p at a distance x_p measured from the one end of the PHP to the centre of the plug as shown in Fig. 6. A net force is exerted on the liquid plug causing it to move. As the liquid plug moves it experiences a shear stress due to friction against the tube walls. A capillary force due to surface tension, and the effect of gravity is also taken into account. Assuming that the PHP is not accelerating a momentum balance on the liquid plug gives

$$m_p \frac{d^2 x_p}{dt^2} = p_{v1} A_c - p_{v2} A_c - \tau_w A_f + m_p g - 4\sigma\left(\cos\theta_r - \cos\theta_a\right)A_c / d_i$$

(4)

where $A_f = \pi d_i L_p$ and $A_c = \pi d_i^2/4$

3. Solution of Equations

Equations (1) to (4) are numerically solved using an explicit finite difference numerical scheme. To solve these equations numerically the PHP is divided into elements of length ΔL each that $L_{tube} = n_{elements} \times \Delta L$. The energy equation for a vapour bubble Eq. (1) in explicit finite difference form is (note that for convenience only the new superscripts $t + \Delta t$ are included in the equations)

$$T_v^{t+\Delta t} = \frac{\Delta t}{m_v c_{vv}}\left(\sum_{k=1}^{n_{wc}} h_{wv} A_v\left(T_w - T_v\right) + \sum_{j=1}^{n_{\ell f}}\left(h_{\ell fv} A_{\ell f}\left(T_{\ell f} - T_v\right) + \dot{m}''_{\ell f} A_{\ell f} i_v\right)\right.$$
$$\left. - \sum_{l=1}^{n_{wm}} \dot{m}''_{wv} A_v i_v - p_v \frac{V_v - V_v^{t-\Delta t}}{\Delta t}\right) + T_v$$

6

(5)

where n_{wc} is the number of areas where heat is transferred from the wall to the vapour

bubble, $n_{\ell f}$ is the number areas where the film is in contact with a vapour bubble and n_{wm} is

the number of dry areas onto which condensation may take place.

The mass flux across the liquid film vapour bubble interface in Eq. (5) is given by

$$\dot{m}''_{\ell f} \propto T_{\ell f} - T_v$$

(6)

and the mass flux for vapour that condenses onto a dry patch on the wall in Eq. (5) is given

by

$$\dot{m}''_{wv} \propto T_v - T_w$$

(7)

(Note that Eq. (7) is only valid if $T_v - T_w > 0$, otherwise $\dot{m}''_{wv} = 0$)

The proportionality term in Eq. (6) and (7) is determined experimentally, but may be

approximated as U/i_{fg} where U is the overall heat transfer coefficient and i_{fg} is the latent heat

of vaporization. For evaporation the latent heat of vaporization is evaluated at saturated

conditions. For condensation, however, the vapour may be superheated. To take the

superheat into account the latent heat of vaporization is given by

$$i_{fg} = \left(i_{fg}\right)_{@\,P_{sat}=P_v} + \bar{c}_{pv}\left(T_v - \left(T_{sat}\right)_{@\,P_{sat}=P_v}\right)$$

(8)

where $\bar{c}_{pv}$ is the specific heat of the vapour at constant pressure and is approximated by

$$\tfrac{1}{2}\left(\left(c_p\right)_{@\,T_v} + \left(c_p\right)_{@\,T_v=T_{sat}\,@\,p_v}\right)$$

For evaporation the enthalpy is evaluated at saturated conditions. However, when condensation takes place the vapour may be superheated so that it is necessary to take the superheat into account. For condensation the enthalpy is given by

$$i_v = (i_v)_{@ \, p_{sat}=p_v} + \overline{c}_{pv}\left(T_v - (T_{sat})_{@ \, p_{sat}=p_v}\right)$$

(9)

The conservation of mass of the film Eq. (2) in explicit finite difference form is

$$m_{\ell f}^{t+\Delta t} = -\dot{m}_{\ell f}''^{t+\Delta t} A_{\ell f} \Delta t + m_{\ell f}$$

(10)

The conservation of mass of the vapour bubble Eq. (3) in explicit finite difference form gives

$$m_v^{t+\Delta t} = \left(\sum_{j=1}^{n_{\ell f}} \dot{m}_{\ell f}''^{t+\Delta t} A_{\ell f} - \sum_{l=1}^{n_{wm}} \dot{m}_{wv}''^{t+\Delta t} A_v\right)\Delta t + m_v$$

(11)

The velocity of the plug is obtained by putting Eq. (4) in explicit finite difference form

$$\dot{x}_p^{t+\Delta t} = \frac{\Delta t}{m_p}\left(p_i A_c - p_{i+1} A_c - \tau_w A_f + m_p g - 4\sigma(\cos\theta_r - \cos\theta_a)A_c/d_i\right) + \dot{x}_p$$

(12)

In Eq. (12) the shear stress between the liquid plug and tube wall is correlated by $\tau_w = C_{fp}\rho_\ell v_p^2/2$ where $C_{fp} = 16/Re$ if $Re = \rho_\ell v_p d_i/\mu_\ell \leq 1180$ otherwise $C_{fp} = 0.078Re^{-0.25}$.

To determine the capillary force experienced by the liquid plug in Eq. (12), values for the advancing and receding contact angles must be known. Information regarding these values is not readily available. A simple relationship will therefore be derived for the capillary forces. The advancing contact angle increases and receding contact angle decreases as the velocity of the liquid plug increases [4][5]. The velocity of a water liquid plug is 492 m/s for a contact angle of $\theta_a = 80°$ at a temperature of 40°C [5]. From experimental observations the velocity

of the liquid plugs is far less than 492 m/s. Taking $\theta_a = 90°$ and $\theta_r = 0°$ at a maximum plug

velocity of $v_{pmax} = 10$ m/s the capillary force will be a maximum $F_{cmax} = 4\sigma A_c/d_i$. For all

other velocities the capillary force is determined by linear interpolation as

$$F_c = 4\sigma(\cos\theta_r - \cos\theta_a)A_c/d_i \approx \frac{F_{c\max}}{v_{p\max}}\dot{x}_p$$

(13)

The plug position is determined from Eq. (12)

$$x_p^{t+\Delta t} = \dot{x}_p\Delta t + x_p$$

(14)

To take into account the interaction of the liquid plug with the liquid film the mass of the

liquid film element is modified depending on how much the plug moved during a time step.

Consider the plug at time t and position x_p^t as shown in Fig. 7(a). From the figure it can be

seen that the second ΔL from the left hand side is partially covered by the liquid plug. The

dashed lines indicate the portion of the ΔL where liquid would have been if it had not been

covered by the liquid plug. The third ΔL is fully covered by the liquid plug and in effect does

not contain any liquid. The first and fourth ΔL is fully exposed to the vapour bubble. As the

plug moves to the new position $x_p^{t+\Delta t}$ as shown in Fig. 7(b), an additional mass of liquid is

deposited at the trailing end of the liquid plug. The total mass of the second ΔL film has

therefore increased. At the leading edge the liquid plug has now crossed a length $x_p^{t+\Delta t} - x_p$

of the fourth element resulting in the decrease of the mass of the fourth element. The mass of

the second liquid film element is modified as follows after the new position of the liquid plug

is known

$$\left(m_{\ell f}^{t+\Delta t}\right)_{\mathrm{mod}} = m_{\ell f}^{t+\Delta t} + \tfrac{1}{4}\pi\rho_\ell\left(d_i^2 - (d_i - 2\delta_{dep})^2\right)\left(x_p^{t+\Delta t} - x_p\right)$$

(15)

The mass of the fourth liquid film element is modified as follows

$$\left(m_{\ell f}^{t+\Delta t}\right)_{\text{mod}} = m_{\ell f}^{t+\Delta t} - \frac{x_p^{t+\Delta t} - x_p^{t}}{\Delta L} m_{\ell f}^{t+\Delta t}$$

(16)

The new volume of each vapour bubble can be determined from the newly calculated plug position of the plugs j and $j+1$, at each end of a vapour bubble as follows

$$V_v^{t+\Delta t} = A_c \left(\left(x_p^{t+\Delta t} - L_p/2 \right)_{j+1} - \left(x_p^{t+\Delta t} - L_p/2 \right)_j \right)$$

(17)

With the volume known the pressure of each vapour bubble can be calculated from the ideal gas law

$$p_v^{t+\Delta t} = \frac{m_v^{t+\Delta t} R_v T_v^{t+\Delta t}}{V_v^{t+\Delta t}}$$

(18)

The process is repeated for the next time step from (5) to (18).

4. Experimental Set-up

The effect of the inclination angle on the heat transfer rate of a closed end PHP as shown in Fig. 8 was experimentally determined. The PHP was constructed from 304 stainless steel tubing and was cast into aluminium to form the condenser and evaporator sections as shown in Fig. 8(b) with $W_e = 110$ mm, $W_a = 80$ mm, $W_c = 110$ mm and $L = 355$ mm. The aluminium thickness of both the evaporator and condenser sections was 25 mm. The total length of the tube in the evaporator is $L_e = 1.957$ m and the total length of the tube in the condenser is $L_c = 1.435$ m. The number of channels is $n_{chan} = 16$. A heating element consisting of electrical resistance wire and insulated with ceramic beads was inserted into the groove as shown in Fig. 8(b) to serve as the heat source. Several cooling channels were drilled through the condenser section through which water flowed from a constant head source to serve as the

10

heat sink. The PHP is mounted onto a stand as shown in Fig. 9. The stand can rotate making it possible for the heat pipe to be rotated in order to evaluate its performance at different inclination angles. The inclination angle is defined as shown in Fig. 10. The inclination angle of the PHP as shown in Fig. 9 is therefore $\phi = 0°$, $\phi = +90°$ would be bottom heat mode and $\phi = -90°$ would be top heat mode. Temperature readings are taken at several locations in the evaporator and condenser sections, as well as the cooling water inlet and outlet using T-type thermocouples. The PHP is filled with de-gassed water liquid to the required charge ratio R. The charge ratio is defined as the ratio of the actual volume of liquid inside the PHP to the total inner volume of the PHP.

5. Comparison of Experimental with Theoretical Results

The closed end stainless steel PHP was numerically modelled using the theoretical model. The values used for the geometry and initial conditions are summarised in Table 1. Refer to Fig. 11 for the definition of the geometry. The geometry of the theoretical model does not match that of the actual model due to the restricted capabilities of the program to divide the PHP into finite elements. The heat transfer rate as a function of the inclination angle predicted by the theoretical model is compared to that experimentally obtained for the PHP with $R = 0.46$ and electrical power input of $\dot{Q}_{elec} = 78$ W in Fig. 12. It can be seen that the theoretically predicted heat transfer rate compares good with the experimental results for -90° $\leq \phi \leq 0°$. The average experimentally determined heat transfer rate for this range of inclination angles is 62 W compared to the theoretically predicted heat transfer rate of 60 W. For $0° < \phi \leq 90°$ the theoretically predicted values are significantly higher than the experimentally determined values. The average experimentally determined heat transfer rate for this range of inclination angles is 65 W compared to the theoretically predicted heat transfer rate of 65 W.

6. Discussion and Conclusions

A theoretical model of a PHP was developed. In the theoretical model the fluid flow is approximated as discrete liquid plugs and vapour bubbles. The theoretical model was used to predict the heat transfer rate of the PHP as a function of the inclination angle and compared to the heat transfer rate experimentally determined. It was found that the theoretically predicted heat transfer rate compared well with the experimental values in the top heat mode ($-90° \leq \phi \leq 0°$) but not as good in the bottom heat mode ($0° < \phi \leq 90°$). The average experimental heat transfer rate in the top heat mode ($-90° \leq \phi \leq 0°$) was 62 W compared to 60 W predicted by the theoretical model. In the bottom heat mode ($0° < \phi \leq 90°$) the average experimental heat transfer rate was 65 W compared to the predicted value of 86 W.

7. References

[1]   Dobson, R. T. and Harms, T. M. Lumped parameter analysis of closed and open oscillatory heat pipes. *11th Int. Heat Pipe Conf*, Tokyo, 12-16 Sept. 1999.

[2]   Swanepoel, G., Taylor, A. B. and Dobson, R. T. Theoretical Modelling of Pulsating Heat Pipes. *Preprints of the 6th International Heat Pipe Symposium*, Chiang Mai, Thailand, 5-9 November 2000.

[3]   Maezawa, S., Izumi, T. and Gi, K. Experimental Chaos in Oscillating Capillary Tube Heat Pipes. *10th Int. Heat Pipe Conf.*, Stuttgart, 21-25 September 1997.

[4]   Kandlikar, S. G., Shoji, M. and Dhir, V. K. *Handbook of Phase Change: Boiling and Condensation*. Taylor & Francis, 1999.

[5]   Friz, G. On the Dynamic Contact Angle in the Case of Complete Wetting. *Z. Angew. Phys*, 19, 374, 1965.
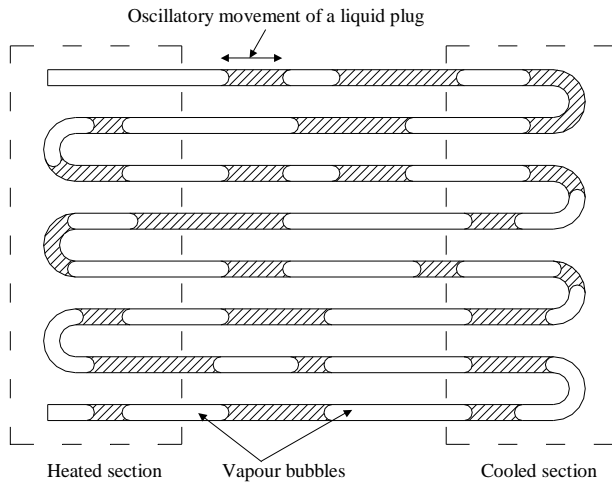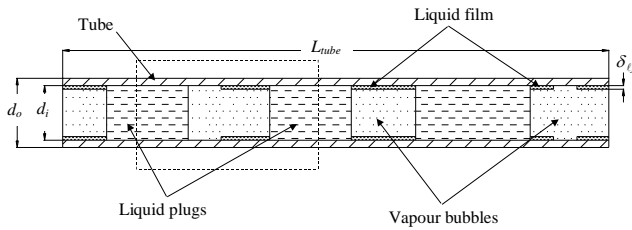
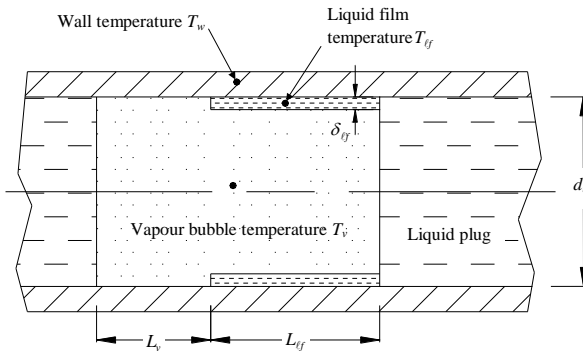Fig. 1 Pulsating heat pipe

Fig. 2 Pulsating heat pipe model

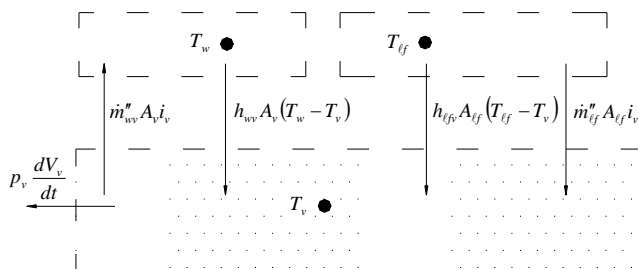Fig. 3 Enlarged view of a vapour bubble with adjacent dry wall and film

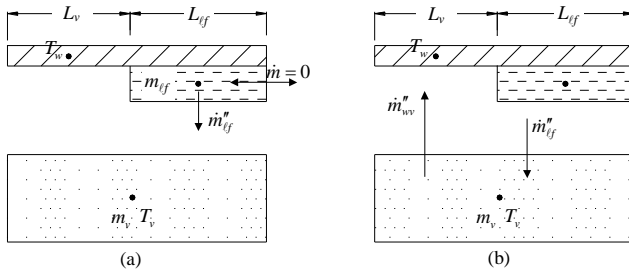Fig. 4 Energy balance on the vapour bubble shown in Fig. 3

13

Fig. 5   Mass balance on the liquid film and the vapour bubble
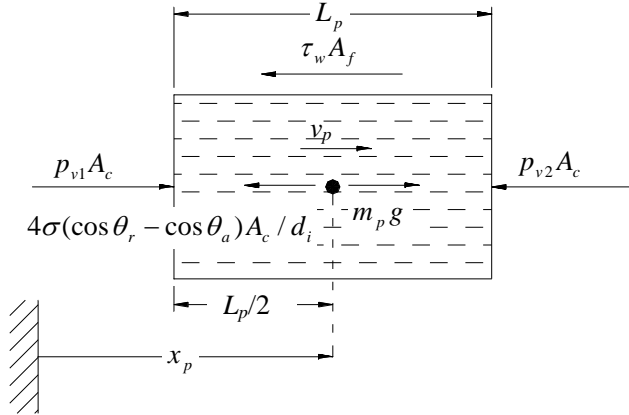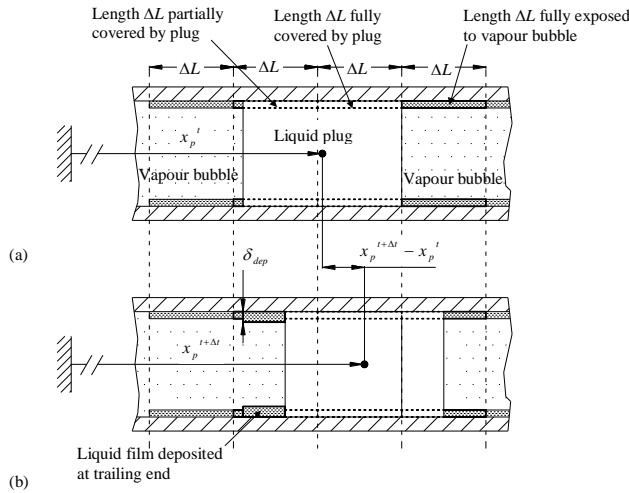

Fig. 6   Momentum balance on a liquid plug

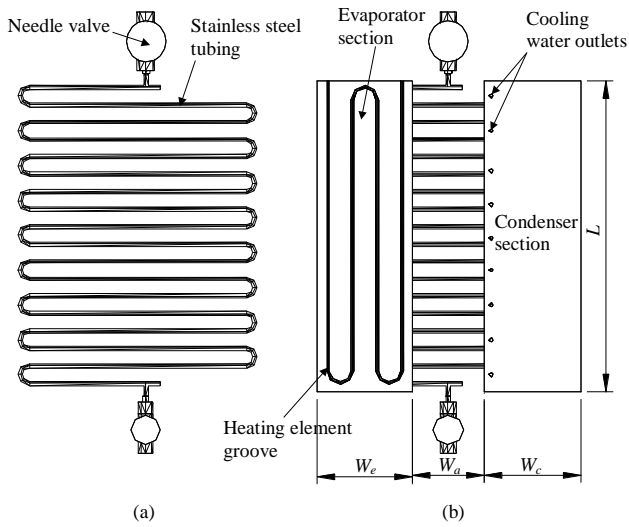Fig. 7   Approximation for the interaction of a liquid plug with the liquid film
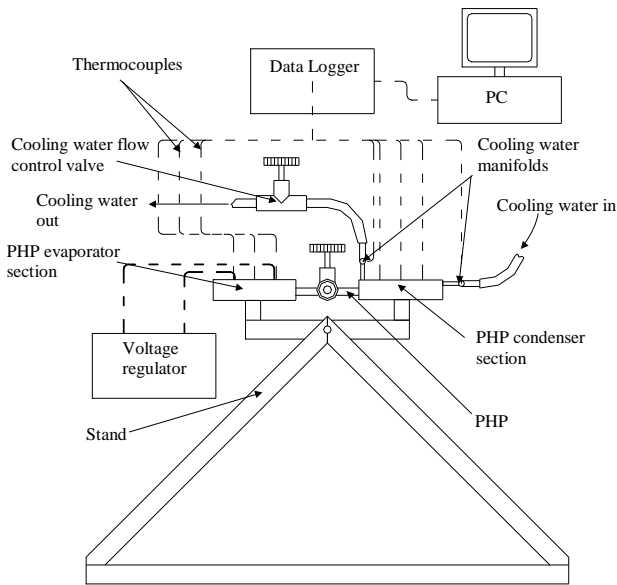
Fig. 8   Stainless steel PHP (4.76mm OD, 3.34mm ID)

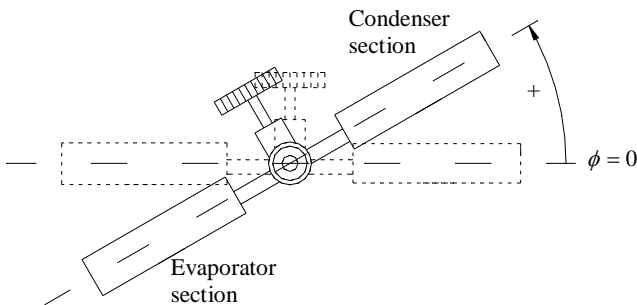Fig. 9   Experimental set-up of a closed end water charged PHP

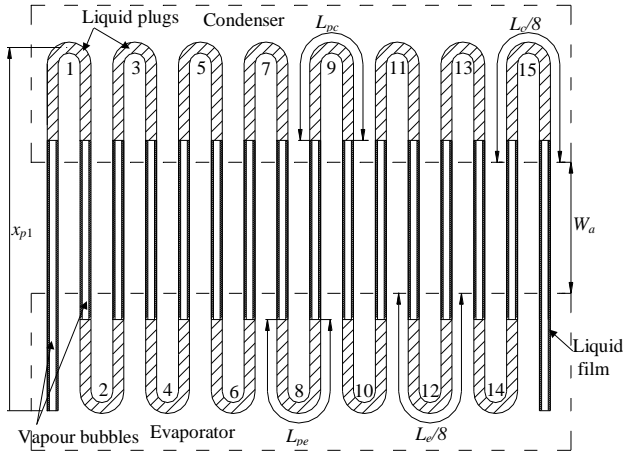Fig. 10 Definition of the inclination (to the horizontal) angle of the PHP

Fig. 11 The definition of the geometry used in the theoretical modelling of the PHP

Table 1　　Initial conditions and geometry used to simulate the PHP

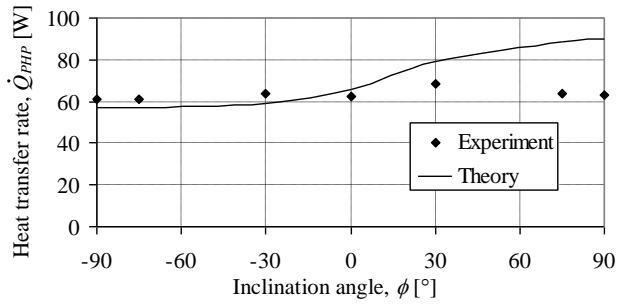|	
$(x_{p0})_i$ (where i is the plug number)	281.25 x i mm
T_{v0}	40 °C
p_{v0}	7238
L_{pe}	135 mm
L_{pc}	140 mm
$L_c/8$	181.125 mm
$L_e/8$	221.375 mm
W_a	80 mm
L_{tube}	4 500 mm
d_i	3.34 mm
T_{we}	60 °C
T_{wc}	40 °C
$\delta_{\ell f}$	0.0001 m
δ_{dep}	0.0001 m
$h_{\ell fw}$ (evaporator and condenser)	800 W/m^{2}K
h_{wv} (evaporator and condenser)	10 W/m^{2}K
$h_{\ell fv}$ (evaporator and condenser)	10 W/m^{2}K
$h_{\ell fw}$, h_{wv}, $h_{\ell fv}$ (adiabatic region)	0 W/m^{2}K

Fig. 12 Comparison of the experimentally determined heat transfer rate with the theoretically predicted heat transfer rate